Electric dipole moments of superheavy elements: A case study on copernicium

Laima Radžiūtė,[1] Gediminas Gaigalas,[1] Per Jönsson,[2] and Jacek Bieroń[3,*]

[1]*Vilnius University, Institute of Theoretical Physics and Astronomy, Saulėtekio av. 3, LT-10222 Vilnius, Lithuania*

[2]*Group for Materials Science and Applied Mathematics, Malmö University, S-20506 Malmö, Sweden*

[3]*Instytut Fizyki imienia Mariana Smoluchowskiego, Uniwersytet Jagielloński, Kraków, Poland*

(Received 20 August 2015; published 14 June 2016)

The multiconfiguration Dirac-Hartree-Fock method was employed to calculate the atomic electric dipole moments (EDMs) of the superheavy element copernicium (Cn, $Z = 112$). The EDM enhancement factors of Cn, calculated here, are about one order of magnitude larger than those of Hg. The exponential dependence of the enhancement factors on the atomic number Z along group 12 of the periodic table was derived from the EDMs of the entire homologous series, Zn, Cd, Hg, Cn, and Uhb. These results show that superheavy elements with sufficiently long half-lives are potential candidates for EDM searches.

DOI: 10.1103/PhysRevA.93.062508

I. INTRODUCTION

The existence of a nonzero permanent electric dipole moment (EDM) of an elementary particle, or in a nondegenerate system of particles, would be one manifestation of violation of parity (P) and time-reversal (T) symmetries [1,2]. Violation of P symmetry has been observed in the β-decay of ^{60}Co [3] followed by decay of muons [4] and pions [5]. Violation of charge and parity (CP) symmetry has been observed in the weak decay of neutral kaons K^0 [6]. Violation of T symmetry is in turn equivalent to violation of combined CP symmetry, through the combined CPT symmetry, which is considered invariant [7]. Both CP- and T-symmetry violations have been observed in the neutral kaon system [8], although direct T-symmetry violation has been disputed [9,10]. More recently a direct observation of the T-symmetry violation in the B-meson system has been reported [11]. The violations of P, C, CP, and T symmetries are predicted by the standard model (SM) of particle physics [12,13]. However, the SM leaves several issues unexplained, such as the origin of baryogenesis, the mass hierarchy of fundamental particles, the number of particle generations, the matter-antimatter asymmetry observed in the universe, and the nature of dark matter. These and other issues are addressed within a large number of extensions of the present version of the SM. Several of these extensions predict EDMs induced by the P- and T-symmetry violating interactions and also EDMs of the fundamental particles significantly larger than the values predicted by the SM itself. The predictions can be tested, and searches for permanent electric dipole moment are under way presently in various systems: neutrons [14], electrons in para- and diamagnetic atoms [15,16], molecules [17,18], and other species [1,19,20]. The experimental searches have not yet detected a nonzero EDM, but they continue to improve the limits on EDMs of individual elementary particles, as well as limits on CP-symmetry violating interactions, parametrized by the coupling constants C_T and C_P (see Refs. [1,21,22] for details, and Table II in Ref. [23] for a summary).

The primary objective of the present paper is the calculation of EDM for the superheavy element copernicium [24,25]. We evaluated the contributions to the atomic EDM induced by four mechanisms [19]: tensor-pseudotensor (TPT) and pseudoscalar-scalar (PSS) interactions, nuclear Schiff moment (NSM), and electron electric dipole moment interaction with the nuclear magnetic field (eEDM). In each case we show that there is an order-of-magnitude increase of atomic EDM between mercury and copernicium. The second objective of the present paper is to derive the Z dependence of the atomic EDM. We show that numerical EDM results are consistent with an exponential Z dependence along the group 12 elements.

II. MCDHF THEORY

We used the multiconfiguration Dirac-Hartree-Fock (MCDHF) approach to generate numerical representations of atomic wave functions. An atomic state function $\Psi(\gamma P J M_J)$ is obtained as a linear combination of configuration state functions $\Phi(\gamma_r P J M_J)$ that are eigenfunctions of the parity P, and total angular momentum operators J^2 and M_J:

$$\Psi(\gamma P J M_J) = \sum_r c_r \Phi(\gamma_r P J M_J). \tag{1}$$

The multiconfiguration energy functional was based on the Dirac-Coulomb Hamiltonian, given (in atomic units) by

$$\hat{H}_{\rm DC} = \sum_{j=1}^{N} [c\boldsymbol{\alpha}_j \cdot \boldsymbol{p}_j + (\beta_j - 1)c^2 + V(r_j)] + \sum_{j<k}^{N} \frac{1}{r_{jk}}, \tag{2}$$

where $\boldsymbol{\alpha}$ and β are the Dirac matrices, and $\boldsymbol{p}$ is the momentum operator. The electrostatic electron-nucleus interaction, $V(r_j)$, was generated from a nuclear charge density distribution $\rho(r)$, which was approximated by the normalized-to-Z two-component Fermi function [26]

$$\rho(r) = \frac{\rho_0}{1 + e^{(r-b)/a}}, \tag{3}$$

where a and b depend on the mass of the isotope. The effects of the Breit interaction, as well as QED effects, were neglected, since they are expected to be small at the level of accuracy attainable in the present calculations.

*Jacek.Bieron@uj.edu.pl

III. MCDHF WAVE FUNCTIONS

We calculated the wave functions of five diamagnetic atoms of group 12, and subsequently the EDMs in the ground states of the entire homologous series, Zn, Cd, Hg, Cn, and Uhb. The numerical representations of the wave functions were generated with the relativistic atomic structure package GRASP2K [27], based on the MCDHF method [26,28–32]. Electron correlation effects were evaluated with methods described in our previous papers [33–36]. Core-valence and valence-valence correlations were included by allowing single and restricted double substitutions to five sets of virtual orbitals. The full description of numerical methods, virtual orbital sets, electron substitutions, and other details of the computations can be found in Ref. [33]. Compared with Ref. [33] the double electron substitutions were, however, extended from the $nsnp$ to the $(n-1)dnsnp$ shells in the present paper (see Sec. V below for details).

IV. EDM CALCULATIONS

An atomic EDM can be written as a sum over states (Eq. (4) in Ref. [33]):

$$d^{\rm int} = 2\sum_i \frac{\langle 0|\hat{D}_z|i\rangle\langle i|\hat{H}_{\rm int}|0\rangle}{E_0 - E_i}, \tag{4}$$

where $|0\rangle$ represents the ground state $|\Psi(\gamma PJM_J)\rangle$ of a closed-shell atom from group 12, with $J=0$ and even parity. The summation runs over excited states $|\Psi(\gamma_i(-P)J_iM_{J_i})\rangle$, with $J_i=1$ and odd parity. E_0 and E_i are energies of ground and excited states, respectively. A calculation of an atomic EDM requires evaluation of the matrix elements of the static dipole $\hat{D}_z$, and the matrix elements of the $\hat{H}_{\rm int}$ interactions, which induce an EDM in an atom [37]. The operator $\hat{H}_{\rm int}$ represents one of the four interactions mentioned in Sec. I above: TPT, PSS, NSM, eEDM:

$$\begin{aligned}
\hat{H}_{\rm TPT} &= i\sqrt{2}G_F C_T \sum_{j=1}^{N}(\langle\boldsymbol{\sigma}_A\rangle\cdot\boldsymbol{\gamma}_j)\,\rho(r_j),\\
\hat{H}_{\rm PSS} &= \frac{-G_F C_P}{2\sqrt{2}m_p c}\sum_{j=1}^{N}\gamma_0(\nabla_j\rho(r_j)\langle\boldsymbol{\sigma}_A\rangle),\\
\hat{H}_{\rm NSM} &= \frac{3}{B}\sum_{j=1}^{N}(\boldsymbol{S}\cdot\boldsymbol{r}_j)\rho(r_j),\\
\hat{H}_{\rm eEDM} &= -id_e\sum_{j=1}^{N}(\boldsymbol{\gamma}_j\boldsymbol{B}).
\end{aligned} \tag{5}$$

where G_F is the Fermi constant, and C_T and C_P are dimensionless constants of TPT and PSS interactions, respectively. The Schiff moment $\boldsymbol{S}$ is directed along the nuclear spin $\boldsymbol{I}$ and $\boldsymbol{S} \equiv S\boldsymbol{I}/I$, where S is the coupling constant with units $|e|\,{\rm fm}^3$, and $B = \int_0^\infty \rho(r)r^4\,dr\,.\,d_e$ represents the electric dipole moment of the electron. More details can be found in Refs. [1,19,38,39]. In order to perform these calculations the GRASP2K package was extended. The extension includes programs for matrix element calculations, based on spin-angular integration [37].

The summation in Eq. (4) involves an infinite number of bound states, as well as contributions from the continuum spectrum. The sum over the bound spectrum was evaluated by explicitly calculating contributions from the lowest five odd states of each symmetry using numerical wave functions. Then the "Riemann ζ tail" method, described in Ref. [33], was applied to sum up the contribution from the remaining bound states. To this end we showed that a summation over a Rydberg series, when extrapolated to large values of the principal quantum number n of the running electron (and where the energy denominator saturates at the ionization energy), converges to the Riemann ζ function. The explicit numerical summation accounts for 98% of the whole sum, and we evaluated the upper bound on the rest (the infinite tail) of the sum by exploiting regularities of the Rydberg series. The relative correction, i.e., the total contribution from the trailing terms (called the Riemann ζ tail) divided by the total contribution from the five leading terms, is of the order of 1.5% for mercury, and less than 2% for copernicium. We neglected the Riemann ζ tail correction for the other three elements (Zn, Cd, and Uhb).

The contribution from the continuum is difficult to estimate, since it is partially accounted for by the virtual set [40]. In the present paper we computed only the contribution of the bound states. We neglected the explicit summation over the continuum and assumed that the continuum spectrum contribution was included in the error budget. The evaluation of the sum over the continuum part of the spectrum could in principle be carried out either fully numerically [41], or again by an extrapolation, based on the fact that the oscillator strength density is continuous across the ionization threshold [42], and the above-mentioned regularities carry over to the continuum spectrum.

The electronic matrix elements in Eq. (4) are not isotope specific, except for a (weak) dependence on radial sizes of nuclei. The radial integrals involved in the calculations of matrix elements of $\hat{H}_{\rm int}$ include factors in the integrands (in the form of nuclear density or nuclear radius; see Eqs. (11)–(23) in Refs. [33]), which effectively cut off the integrals outside the nuclear radius. Also, the atomic wave functions do exhibit (also weak) dependence on atomic mass, through the nuclear electrostatic potential, which depends on the nuclear charge density distribution, which in turn depends on the nuclear mass number, through Eq. (3) above. All numerical results in the present paper were obtained for specific isotopes, $^{69}_{30}$Zn, $^{111}_{48}$Cd, $^{199}_{80}$Hg, $^{285}_{112}$Cn, and $^{482}_{162}$Uhb, and therefore they do exhibit a dependence on atomic masses. However, the dependence is negligibly weak – well below the accuracy attainable in the present calculations. Therefore, these results may also be used for other isotopes of the above elements.

V. MERCURY

The calculations for mercury were performed in a similar manner as those presented in our previous paper [33]. The Dirac-Fock (DF) results and results from calculations with the first two layers of virtual orbitals (i.e., the first three lines in Tables I, II, III, and IV) are in fact identical with the results published in Ref. [33]. Further calculations differ in the scope

TABLE I. TPT interaction contributions to EDM in different virtual sets, in units ($10^{-20} C_T \langle \sigma_A \rangle |e|$cm), for Zn, Cd, Hg, and Cn, compared with data from other methods. See text for explanation and details.

	Zn		Cd		Hg		Cn		
VOS	Th	SE	Th	SE	Th	SE	Th	Th2	Th3
DF	−0.07	−0.07	−0.35	−0.36	−7.29	−6.15	−59.86	−61.50	−66.66
1	−0.08	−0.09	−0.39	−0.45	−4.13	−4.86	−48.53	−50.95	−53.95
2	−0.09	−0.11	−0.45	−0.54	−4.66	−5.23	−58.38	−58.92	−62.96
3	−0.10	−0.12	−0.47	−0.57	−4.84	−5.53	−59.31	−64.53	−68.76
4	−0.10	−0.12	−0.48	−0.59	−4.79	−5.64	−57.67	−61.04	−65.26
5	−0.11	−0.12	−0.49	−0.60	−4.84	−5.64	−57.51	−60.75	−64.98
Ref. [38] (DHF)						−2.4			
Ref. [43] (DHF)						−2.0			
Ref. [38] (CI+MBPT)						−5.12			
Ref. [38] (RPA)						−5.89			
Ref. [43] (RPA)						−6.0			
Ref. [44] (CPHF)						−6.75			
Ref. [45] (CCSD)						−4.3			

of the double electron substitutions, which were extended from $6s6p$ to $5d6s6p$ shells.

The results of the calculations are presented in Tables I, II, III, and IV. The number of virtual orbital sets (VOSs) is listed in the first column of each table (see Chap. III of Ref. [33] for definitions and for the details of the calculations). The row marked DF in the VOS column represents the lowest-order approximation, with zero sets of virtual orbitals. It should be noted that the values in the tables marked DF and DHF (Dirac-Hartree-Fock) are not equivalent. Those marked DF were obtained in the present calculations with only the two lowest excited states included in the summation in Eq. (4). The results marked "DHF," obtained with many-body perturbation theory (MBPT) methods, involved summation over the entire spectrum of virtual orbitals using various methods to construct the virtual orbital set [38,43,48]. Neither DF nor DHF includes electron correlation effects and therefore they are relevant only for the purpose of evaluating the contributions of electron correlation for the expectation values of interest. A larger number of VOSs represents in principle a better approximation of the wave function. The row marked 5 in the VOS column represents the final approximation, with five sets of virtual orbitals (MCDHF-VOS.5, represented by red circles in Fig. 2). The difference between VOS.4 and VOS.5 may (cautiously) be taken as an indication of accuracy. For each element the calculated values of the energy denominators in Eq. (4) were used to evaluate the atomic EDMs. These fully theoretical EDM values are marked "Th" in Tables I, II, III, and IV. Semiempirical EDM values (marked "SE" in the tables) were also evaluated for Zn, Cd, and Hg, with the energy denominators taken from the NIST database [49]. Level identifications were made with the atomic state functions transformed from jj coupling to the LSJ coupling scheme, using the methods developed in Refs. [50,51].

VI. COPERNICIUM

Three different sets of energy denominators for copernicium were used. Those from the present calculations are marked "Th." For comparison purposes we computed also the EDMs with the energy denominators taken from two other theoretical papers [52,53]. The results in the column marked "Th2" were obtained with the energy denominators taken from Ref. [52], which used a large-scale MCDHF method. The authors of Ref. [52] evaluated also the ionization limit of copernicium, and their calculated ionization energy was used

TABLE II. PSS interaction contributions to EDM in different virtual sets, in units ($10^{-23} C_P \langle \sigma_A \rangle |e|$cm), for Zn, Cd, Hg, and Cn, compared with data from other methods. See text for explanation and details.

	Zn		Cd		Hg		Cn		
VOS	Th	SE	Th	SE	Th	SE	Th	Th2	Th3
DF	−0.13	−0.14	−0.94	−0.96	−25.47	−21.49	−199.52	−252.66	−274.11
1	−0.15	−0.17	−1.05	−1.21	−14.54	−17.16	−199.52	−209.13	−221.73
2	−0.19	−0.23	−1.19	−1.46	−16.38	−18.39	−240.22	−242.15	−259.07
3	−0.20	−0.24	−1.25	−1.53	−17.01	−19.47	−244.96	−266.95	−284.65
4	−0.20	−0.24	−1.28	−1.58	−16.84	−19.84	−237.56	−251.33	−268.95
5	−0.22	−0.24	−1.30	−1.60	−17.02	−19.85	−236.88	−250.07	−267.78
Ref. [38] (DHF)						−8.7			
Ref. [38] (CI+MBPT)						−18.4			
Ref. [38] (RPA)						−20.7			

TABLE III. Schiff moment contributions to atomic EDM in different virtual sets, in units $\{10^{-17}[S/(|e|\mathrm{fm}^3)]|e|\mathrm{cm}\}$, for Zn, Cd, Hg, and Cn, compared with data from other methods. See text for explanation and details.

	Zn		Cd		Hg		Cn		
VOS	Th	SE	Th	SE	Th	SE	Th	Th2	Th3
DF	−0.04	−0.04	−0.18	−0.19	−2.86	−2.46	−17.73	−17.26	−19.53
1	−0.05	−0.06	−0.21	−0.26	−1.95	−2.45	−13.64	−12.96	−14.53
2	−0.06	−0.07	−0.25	−0.32	−2.11	−2.42	−17.05	−15.96	−17.78
3	−0.06	−0.08	−0.27	−0.34	−2.21	−2.58	−20.09	−22.66	−24.58
4	−0.06	−0.08	−0.28	−0.35	−2.19	−2.62	−17.75	−18.02	−19.95
5	−0.07	−0.08	−0.28	−0.35	−2.22	−2.63	−17.62	−17.77	−19.71
Ref. [38] (DHF)						−1.2			
Ref. [38] (CI+MBPT)						−2.63			
Ref. [38] (RPA)						−2.99			
Ref. [46] (CI+MBPT)						−2.8			
Ref. [47] (TDHF)						−2.97			
Ref. [45] (CCSD)						−5.07			

in our evaluation of EDMs for those levels which were not reported in Ref. [52]. The energy denominators in the columns marked "Th3" were taken from Ref. [53], where the energy spectrum was computed with two methods: configuration interaction (CI) and CI+MBPT. We gave priority to the CI+MBPT results; the CI results were used when CI+MBPT data were not available. For the remaining levels the energy denominators were replaced by the calculated ground-state ionization energy. The accuracy of our calculated energy values, as well as those from Refs. [52,53], is better than 20% for the lowest excited levels of mercury.

The mass number 285 for the element Cn was chosen due to predictions that heavier isotopes are more stable than lighter ones [54,55]. The lifetimes of several known isotopes of Cn are counted in minutes [56], which make them amenable to atom traps, and subsequent spectroscopy. It is predicted that still heavier isotopes of Cn, with mass numbers in the range 290–294, may have half-lives counted in years [55].

We observed a similar pattern of contributions from individual electronic states, as described in Ref. [33]. The triplet $6snp\ ^3P_1$ and the singlet $6snp\ ^1P_1$ states are the dominant contributors to atomic EDM in the Hg spectrum. For the Cn case the dominant contributions arise from the lowest states of $^{1,3}P_1$ symmetries, i.e., $7snp\ ^1P_1$, $7snp\ ^3P_1$. Altogether they contribute in excess of 98% of the total EDM. The remaining Rydberg states contribute less than 2%. Instead of an explicit error analysis for the calculations of EDM for copernicium we applied a comparison with mercury. Estimates of the magnitudes of EDMs induced by the TPT, PSS, NSM, and eEDM mechanisms in mercury have been performed with several theoretical methods [38,44,45,47]. With one or two exceptions [45,57], they all agree within reasonable error bounds – of the order of 10–20 % [33]. The results of the MCDHF calculations for mercury, both in the present paper as well as in Ref. [33], are well within these bounds. We expect that the present calculations for copernicium, performed with the same MCDHF model as those for mercury, would also fit within error bounds of similar size.

VII. UNHEXBIUM

In addition to the calculations described above we have done uncorrelated DF calculations for the element Unhexbium

TABLE IV. Contributions of electron EDM interaction with magnetic field of nucleus, to atomic EDM in different virtual sets, in units $(d_e \times 10^{-4})$, for Zn, Cd, Hg, and Cn, compared with data from other methods. See text for explanation and details.

	Zn		Cd		Hg		Cn		
VOS	Th	SE	Th	SE	Th	SE	Th	Th2	Th3
DF	0.13	0.14	−0.62	−0.63	16.04	13.41	314.03	324.40	350.09
1	0.11	0.09	−0.64	−0.71	8.47	9.58	254.78	269.22	283.51
2	0.13	0.13	−0.69	−0.81	9.63	10.64	305.55	309.48	328.86
3	0.14	0.14	−0.72	−0.85	9.99	11.30	305.13	329.18	349.47
4	0.14	0.14	−0.73	−0.87	9.90	11.53	300.39	318.41	338.60
5	0.13	0.11	−0.75	−0.88	10.00	11.50	299.67	317.11	337.40
Ref. [38] (DHF)						4.9			
Ref. [48] (DHF)						5.1			
Ref. [38] (CI+MBPT)						10.7			
Ref. [38] (RPA)						12.3			
Ref. [48] (RPA)						13			

(E162) and for beryllium. There are several theoretical predictions [58–60] which suggest that the heaviest homolog in the Zn-Cd-Hg-Cn-U*xx* group would not be element E162 (Unhexbium), but E164 (Unhexquadium). Due to a very large spin-orbit splitting of the $8p$ shell, the relativistic $8p_{1/2}$ shell becomes occupied before the $7d$ shell is filled [60]. Therefore, at the end of the transition metals in row eight of the periodic table there appears the element E164, with the ground configuration $[\mathrm{Cn}]5g^{18}6f^{14}7d^{10}7p^{6}8s^{2}8p^{2}$, with all inner shells closed, and with two electrons in the $8p_{1/2}$ shell (the $8p_{1/2}$ shell is, in fact, also closed). However, the presence of the $8p$ shell would complicate the calculations of EDMs, and, more importantly, it would complicate comparisons along the homologous series. Therefore, we have deliberately chosen (a doubly artificial) isotope $^{482}_{162}$Uhb, of element E162 (Unhexbium) with electron configuration $[\mathrm{Cn}]5g^{18}6f^{14}7d^{10}7p^{6}8s^{2}$.

VIII. *Z* DEPENDENCE

Atomic properties depend in various ways on the atomic number Z, both in isoelectronic sequences [61–64] as well as along homologous sequences [65,66]. In many cases approximate analytic relations were derived [61,64–66], and several atomic observables exhibit a polynomial or power dependency on the atomic number Z.

Atomic enhancement factors of the PT-odd interactions in neutral atoms scale with nuclear charge as $d_{\mathrm{at}} \sim \alpha^2 Z^3$. The factor Z^3 arises from an estimate of the strength of the electric field in the vicinity of an atomic nucleus (see Chap. 6.2 of Ref. [1]), but it has been pointed out that on top of the Z^3 enhancement of the PT-odd interaction there is another enhancement factor, arising from relativistic contraction of the electronic wave function [1,39,67–71]:

$$K_r \approx \left(\frac{\Gamma(3)}{\Gamma(2\gamma+1)}\right)^2 \left(\frac{2Zr_N}{a_0}\right)^{2\gamma-2}. \tag{6}$$

Z dependence of atomic EDMs induced by the (P,T)-odd $\hat{H}_{\mathrm{int}}$ interactions is governed by the Z dependence of three factors in Eq. (4): the matrix element of the (P,T)-odd $\hat{H}_{\mathrm{int}}$ operator, the matrix element of the electric dipole $\hat{D}_z$ operator, and the energy denominator $(E_0 - E_i)$. The matrix elements of the electric dipole $\hat{D}_z$ operator are constrained by the Thomas-Reiche-Kuhn rule. In the case of the elements of group 12 they are further constrained by the Wigner-Kirkwood sum rule (see Chap. 14 of Ref. [65]). The two lines, $ns^2\,{}^1S_0$–$nsnp\,{}^3P_1$ and $ns^2\,{}^1S_0$–$nsnp\,{}^1P_1$, dominate the Wigner-Kirkwood sum in all five elements, making the matrix element of $\hat{D}_z$ approximately constant along the homologous series. Transition energy denominators in Eq. (4) do not depend on Z along the homologous series [66], except for small variations due to shell contractions, shell rearrangements, etc. (excluding the Uhb element, with its large spin-orbit splitting mentioned in Sec. VI above).

Therefore, the dominant role in establishing the Z dependence of atomic EDMs along the homologous sequence is taken by the $\hat{H}_{\mathrm{int}}$ operators. Following the analysis in Chap. 8 of Ref. [1], it can be shown that in the vicinity of a pointlike atomic nucleus the large $P_{n\kappa}$ and small $Q_{n\kappa}$ radial components

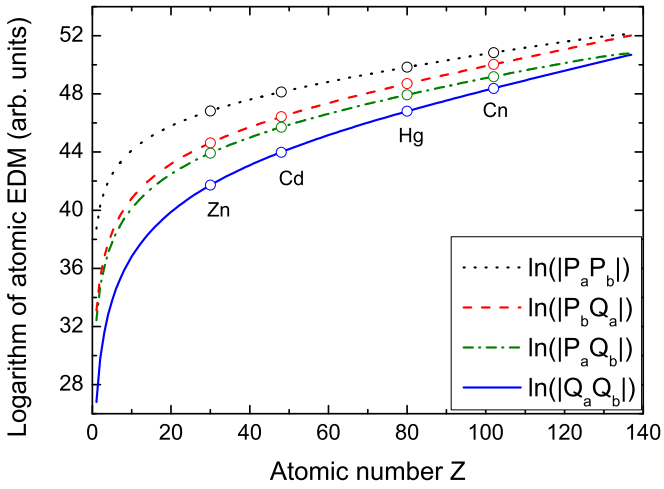

FIG. 1. Z dependence of the atomic EDM. The right-hand side of Eq. (9), calculated from (absolute values of) one-electron wave function factors P_aP_b, Q_aQ_b, P_aQ_b, and P_bQ_a. The factors were generated from Eqs. (7) and (8), and evaluated at $r = r_N$, as functions of atomic number Z. See text for details.

of a one-electron wave function may be expressed as

$$P_{n\kappa}(r) = \frac{\kappa}{|\kappa|}(\kappa-\gamma)\left(\frac{Z}{a_0^3\nu^3}\right)^{1/2}\frac{2}{\Gamma(2\gamma+1)}\left(\frac{a_0}{2Zr}\right)^{1-\gamma}, \tag{7}$$

$$Q_{n\kappa}(r) = \frac{\kappa}{|\kappa|}(Z\alpha)\left(\frac{Z}{a_0^3\nu^3}\right)^{1/2}\frac{2}{\Gamma(2\gamma+1)}\left(\frac{a_0}{2Zr}\right)^{1-\gamma}, \tag{8}$$

where κ is the angular momentum quantum number, $\gamma^2 = \kappa^2 - \alpha^2Z^2$, α is the fine structure constant, ν^3 is the effective principal quantum number, and a_0 is the Bohr radius. The radial integrals involved in the calculations of matrix elements of $\hat{H}_{\mathrm{int}}$ include the integrands of the combinations of the large $P_{n\kappa}$ and small $Q_{n\kappa}$ radial components, of the type $(P_aP_b \pm Q_aQ_b)$ or $(P_aQ_b \pm P_bQ_a)$. All these integrals include factors in the integrands which effectively cut off the integrals outside the nucleus [33], and eventually Z dependence of the atomic EDM in the form

$$d_{\mathrm{at}} \sim \left(\frac{Z^k}{a_0^3\nu^3}\right)\left(\frac{2}{\Gamma(2\gamma+1)}\right)^2\left(\frac{2Zr_N}{a_0}\right)^{2\gamma-2} \tag{9}$$

is obtained, where k depends on a particular form of the integrand and where r_N is the effective cutoff radius. The right-hand side of Eq. (9) is displayed in Fig. 1. All four combinations $(P_aP_b, Q_aQ_b, P_aQ_b,$ and $P_bQ_a)$ of the one-electron wave function factors from Eqs. (7) and (8) are represented as functions of atomic number Z. The index a represents $ns_{1/2}$ orbitals, and the index b represents $np_{3/2}$ orbitals. The nuclear radius r_N has been computed using $r_N = r_0A^{1/3}$, where $r_0 = 1.25$ fm. The relation of atomic mass A to atomic number Z has been evaluated from the neutron-to-proton ratio $N/Z = 1 + A^{2/3}a_C/2a_A$, derived from the Bethe-Weizsäcker formula [72], with $a_C = 0.711$ and $a_A = 23.7$. The open circles in Fig. 1 show positions of the four elements (Zn, Cd, Hg, and Cn) considered in this paper.

Neglecting a weak Z dependence through the Γ function $2/\Gamma(2\gamma+1)$, for small values of Z the polynomial factor Z^k determines the functional form of the dependence on Z

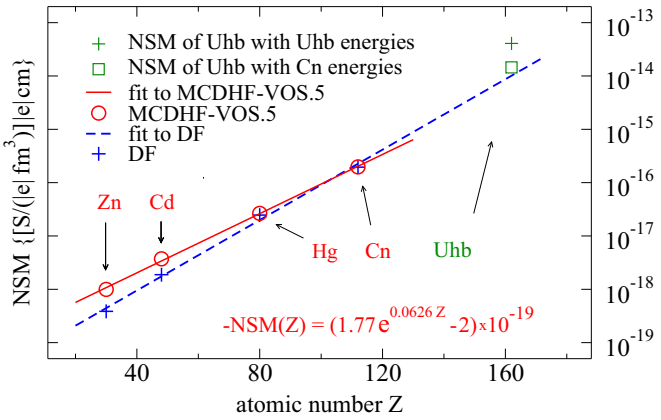

FIG. 2. Atomic EDM (absolute values) induced by the NSM as a function of atomic number Z. Red circles are MCDHF-VOS.5 results with five virtual orbital sets. Blue pluses are uncorrelated DF results (zero sets). The lines are exponential functions fitted to the four points, representing Zn, Cd, Hg, and Cn. The solid red line is the fit to MCDHF-VOS.5 results. The dashed blue line is the fit to uncorrelated DF results. The lines are extrapolated beyond $Z = 112$. The two symbols in the upper right corner represent Uhb (excluded from the fitting). The green plus is the DF result for Uhb with calculated Uhb energy denominators. The green square is the DF result for Uhb with energy denominators taken from Cn. The sizes of circles represent approximately the relative accuracy of the MCDHF-VOS.5 calculations. See text for details.

while for large values of Z the exponential factor $(2Zr_N)^{2\gamma-2}$ takes over. It can be shown numerically, as can be seen in Fig. 1, that the polynomial Z^k shape dominates up to about $Z = 60$, then in the range $60 < Z < 120$ the function $d_{\rm at}(Z)$ is approximately exponential, and eventually the approximation breaks down, because the analytic approximation in Eqs. (7) and (8) is valid only within the atomic number Z range, where bound solutions of the Dirac equation exist ($Z \leqslant 137$ for pointlike nuclei).

The analysis above has been made under the assumption of a pointlike Coulomb field in the Dirac radial equation. The finite sizes of nuclei entered only when Eq. (9) was evaluated. For extended nuclei the solution of the Dirac equation depends on the specific form of the nuclear charge distribution [32,73,74]. Flambaum and Ginges [39] and Dzuba *et al.* [21] assumed uniform distribution of the electric charge inside a sphere (with the normalization factors from Ref. [71]) and obtained enhancement factors of a similar form as in Eqs. (6) and (9), for angular symmetries $s_{1/2}$, $p_{1/2}$, and $p_{3/2}$.

In the present paper the numerical calculations for the homologous series of group 12 of the periodic table (Zn, Cd, Hg, Cn, and Uhb) were performed with extended nuclear model (3), for which bound solutions of the Dirac-Fock equations exist up to $Z = 173$ [75]. The dependence of EDMs on atomic number Z along group 12 of the periodic table is presented in Fig. 2. The red circles represent our final results, calculated within the MCDHF-VOS.5 electron correlation model described above. The blue pluses represent the uncorrelated DF results. The green plus in the upper right corner represents the EDM value for Uhb. Due to very large spin-orbit splitting of the $8p$ shell (see Sec. VI above), the Uhb energy denominators are distinctively different from those of other members of the homologous series. To compensate for this splitting, we also computed the EDMs for Uhb with energy denominators taken from Cn. The latter value is represented by the square in Fig. 2. The solid line is fitted to the four (Zn, Cd, Hg, and Cn) final results. The dashed line is fitted to the four uncorrelated DF results. The Uhb results were excluded from the fitting. The regression analysis yields the following relations:

$$
\begin{aligned}
d^{\rm TPT} &= \left[-1.22(8)e^{0.0766(6)Z} - 5(6)\right] \times 10^{-22},\\
d^{\rm PSS} &= \left[-30(1)e^{0.0813(3)Z} - 8.54(1)\right] \times 10^{-26},\\
d^{\rm NSM} &= \left[-1.77(7)e^{0.0626(3)Z} + 2(2)\right] \times 10^{-19},\\
d^{\rm eEDM}/\mu &= \left[2.74(8)e^{0.0841(2)Z} - 15(9)\right] \times 10^{-6}, \qquad (10)
\end{aligned}
$$

where the numbers in parentheses represent root-mean-square-error deviations. The third line of Eq. (10) is displayed in Fig. 2.

Similar regression analysis can be done for the semianalytic relations presented for the point-nucleus case in Eq. (9) and in Fig. 1, but restricted to the range of atomic numbers $30 \leqslant Z \leqslant 112$, covered by the four elements (Zn, Cd, Hg, and Cn) considered in this paper. The analysis yields $d^{\rm PSS} \sim e^{0.017Z}$ and $d^{\rm NSM} \sim e^{0.022Z}$, somewhat smaller exponents than those presented in Eq. (10).

The deviation of the EDM value for element E162 from the fitted function in Fig. 2 may be explained by several possible mechanisms: rearrangements of the valence shells, i.e., relativistic contraction of the $8s$ and $8p_{1/2}$ shells, which results in the above-mentioned large spin-orbit splitting of the $8p$ shell; variation of transition energy denominators, induced by shell rearrangements; and contribution of QED effects, which could be quite sizable near the end of the periodic table at $Z = 173$ [75,76]. However, the most likely explanation is the breakdown of the exponential approximation near the end of the periodic table. The analytic approximation in Eqs. (7) and (8) is valid only within the atomic number Z range, where bound solutions of the Dirac equation exist ($Z \leqslant 137$ for pointlike nuclei, $Z \leqslant 173$ for extended nuclei). The element E162 is close to the end of the periodic table at $Z = 173$, where determination of a numerical wave function, even at the Dirac-Fock level, may be problematic or impossible, and one might expect a question whether perturbation theory still works in QED for elements close to $Z = 173$ [75].

At very short distances Z-dependence algebra is dominated by the cutoff radii r_N (related to the sizes of the nuclei) and by the power-series solutions for $P_{n\kappa}$ and $Q_{n\kappa}$ at the origin [32]. The power-series coefficients for $P_{n\kappa}$ and $Q_{n\kappa}$ depend on the nuclear potential (again related to the sizes of the nuclei) and are constrained by orthogonality of the one-electron functions with the same symmetry. The dominant contributions to the matrix elements of the $\hat{H}_{\rm int}$ operators come from the valence ns^2 orbitals in the ground state, and from the lowest $np_{1/2}$ and $np_{3/2}$ orbitals in the excited states.

The upper graph in Fig. 3 shows the coefficient p_0 of the lowest-order polynomial in the series expansion at the origin of the large component P of the radial function of the valence orbitals (ns, $np_{1/2}$, $np_{3/2}$) of the elements from group 12 (plus beryllium). The quantum number n assumes the values 2, 4, 5, 6, 7, and 8 for Be, Zn, Cd, Hg, Cn, and Uhb, respectively. The lower graph in Fig. 3 shows the atomic EDMs induced by the TPT, PSS, NSM, and eEDM mechanisms, as functions

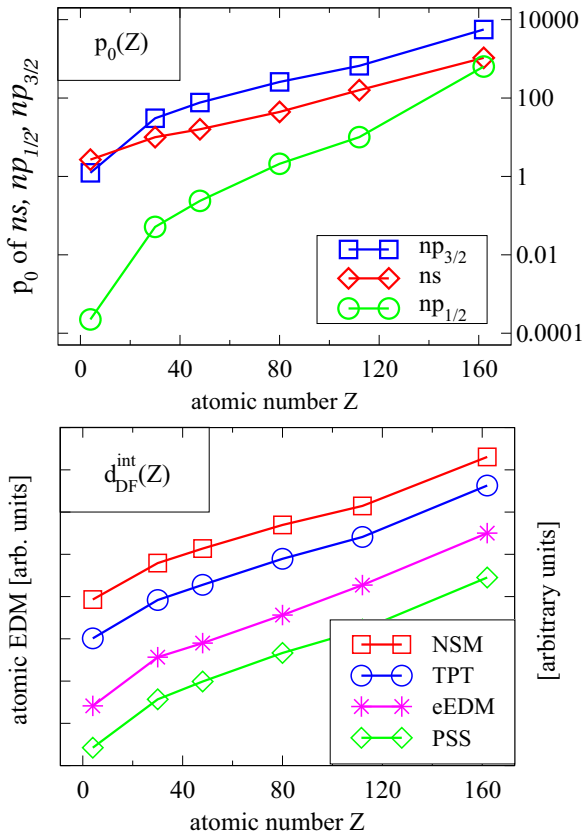

FIG. 3. Top: Power-series coefficients p_0 of valence orbitals as functions of atomic number Z. Blue squares, $np_{3/2}$; red diamonds, ns; green circles, $np_{1/2}$; $n = 2, 4, 5, 6, 7$, and 8 for Be, Zn, Cd, Hg, Cn, and Uhb, respectively. Bottom: Atomic EDM (in arbitrary units on logarithmic scale), induced by NSM (red squares), TPT (blue circles), eEDM (magenta stars), and PSS (green diamonds), as a function of atomic number Z. All lines in both graphs are drawn only as guidance for the eyes. See text for details.

of atomic number Z for the elements of group 12 (plus Be). For the purpose of this comparison, all values in Fig. 3 were obtained in the Dirac-Fock approximation, without account of electron correlation effects, and with the extended nuclear model (3). Analogously to the point nucleus case [represented by Eq. (9)], the function $d_{\rm at}(Z)$ is approximately exponential in the range $60 < Z < 120$, i.e., for heavy and superheavy elements relevant from the point of view of the EDM searches. Both graphs in Fig. 3 show similar Z dependencies as those in Fig. 1, i.e., the polynomial shape up to about $Z = 60$, then approximately exponential in the range $60 < Z < 120$, and eventually the exponential approximation breaks down near the end of the extended Periodic Table of Elements [60,75] at $Z = 173$. When comparing the shapes of the curves in the upper and lower graphs, one has to bear in mind that radial integrals in matrix elements of the $\hat{H}_{\rm int}$ operators involve valence ns^2 orbitals in the ground state, and $np_{1/2}$ and $np_{3/2}$ orbitals in the excited states. The apparent similarity of the $np_{1/2}$ and $np_{3/2}$ curves in the upper graph and the four curves in the lower graph is a numerical confirmation of the dominant role of power-series coefficients in the matrix element of the $\hat{H}_{\rm int}$ operators, as well as of the proportionality relations between matrix elements, established in Ref. [21]. Beryllium does not belong to group 12 (which results in the visible deviation of Be from the fitted function) but was included in Fig. 3 to indicate that the dominant role of power-series coefficients, as well as the proportionality relations [21], is not limited to one group of elements. The other deviations from linearity in the Fig. 3 are induced by electron correlation effects, whose contributions differ from element to element due to shell rearrangements.

IX. CONCLUSIONS

EDMs have not yet been detected experimentally. The experimental searches have been going on for the past 50 years, and the role of theory is not only to provide limits on the fundamental parameters but also to guide the experimentalists to atoms, molecules, and other systems with suitable enhancement factors. Experimentalists need to know (the order of magnitude of) enhancement factors before they set up their apparatus to detect EDM in a new species [2,77]. The present paper is intended to present the calculations of EDMs, carried out with the multiconfiguration Dirac-Hartree-Fock theory, of the superheavy element copernicium. The main conclusion of the present paper is the suggestion for setting up an EDM experiment on a superheavy element, which would result in an order-of-magnitude increase of sensitivity, compared to a homologous heavy element. Such homologous pairs include (but are not limited to) Yb-No, Hg-Cn, Tl-E113, Po-Lv, At-E117, Rn-E118, Fr-E119, and Ra-E120. If the exponential Z dependence derived in the present paper is assumed for all above homologous pairs, an increase of sensitivity by a factor of 8–30 should be expected. The best limit on the EDM of a diamagnetic atom comes from ^{199}Hg, for which $d(^{199}\mathrm{Hg}) < 3.1 \times 10^{-29}\, e\,$cm (95% C.L.) has been reported [16]. Our calculations indicate that for the Hg-Cn pair the increase of sensitivity would be 57.5/4.8, 236.9/17.0, 17.6/2.2, and 299.7/10.0 for TPT, PSS, NSM, and eEDM, respectively. Over the past 50 years the precision of EDM experiments has been improving by about an order of magnitude per decade [2,16,18,23,78,79]. On this timescale an experiment on Cn would be equivalent to time travel into the future over a distance of about 10 to 20 years.

We are of course aware of the fact that an EDM experiment on a short-lived superheavy element is impractical at this time. However, the techniques for trapping atoms [80,81], controlling quantum systems [82,83], and performing spectroscopic investigations of radioactive [84] and superheavy elements [85] advance rapidly. At the same time the quest for the superheavy island of stability continues [55,86], and sooner or later one may expect a breakthrough of laser spectroscopic methods into the realm of superheavy elements [85].

EDM experiments with superheavy elements, if they ever become feasible, would probably constitute the final frontier for atomic tests of violation of parity (P) and time-reversal (T) symmetries. In recent years the molecular avenue promises to become more competitive in EDM searches. The advantage of molecular eEDM experiments is in the large values of the effective electric field, several orders of magnitude higher than those in atoms [17,18,87,88]. Current progress in cooling and trapping molecules [89–93], as well as molecular ions [94,95],

may soon allow one to increase coherence times and improve population control in molecular experiments, which might translate into a significant advantage of molecular experiments over atomic ones.

While an EDM experiment on a short-lived superheavy element is impractical at this time, still less practical would be an experiment on a superheavy molecule. However, when molecular EDM experiments become feasible, one may also envisage making, trapping, and eventually performing spectroscopy of superheavy molecules. It is difficult to say what is impossible, for the dream of yesterday is the hope of today and the reality of tomorrow [96].

ACKNOWLEDGMENTS

L.R. is thankful for the HPC resources provided by the ITOAC of Vilnius University. J.B., G.G., and P.J. acknowledge the support from the Polish Ministry of Science and Higher Education (MNiSW) in the framework of Grant No. N N202 014140 awarded for the years 2011–2016. J.B. acknowledges the support from the European Regional Development Fund in the framework of the Polish Innovation Economy Operational Program (Contract No. POIG.02.01.00-12-023/08). P.J. acknowledges financial support from the Swedish Research Council under Grant No. 2015-04842.

[1] I. B. Khriplovich and S. K. Lamoreaux, *CP Violation Without Strangeness* (Springer, Berlin, 1997).
[2] K. Jungmann, Ann. Phys. **525**, 550 (2013).
[3] C. S. Wu, E. Ambler, R. W. Hayward, D. D. Hoppes, and R. P. Hudson, Phys. Rev. **105**, 1413 (1957).
[4] R. L. Garwin, L. M. Lederman, and M. Weinrich, Phys. Rev. **105**, 1415 (1957).
[5] J. I. Friedman and V. L. Telegdi, Phys. Rev. **106**, 1290 (1957).
[6] J. H. Christenson, J. W. Cronin, V. L. Fitch, and R. Turlay, Phys. Rev. Lett. **13**, 138 (1964).
[7] V. A. Kostelecky and N. Russell, Rev. Mod. Phys. **83**, 11 (2011).
[8] A. Angelopoulos, A. Apostolakis, E. Aslanides, G. Backenstoss, P. Bargassa, O. Behnke, A. Benelli, V. Bertin, F. Blanc, P. Bloch, P. Carlson, M. Carroll, E. Cawley, S. Charalambous, M. Chertok, M. Danielsson, M. Dejardin, J. Derre, A. Ealet, C. Eleftheriadis, L. Faravel, W. Fetscher, M. Fidecaro, A. Filipčič, D. Francis, J. Fry, E. Gabathuler, R. Gamet, H.-J. Gerber, A. Go, A. Haselden, P. Hayman, F. Henry-Couannier, R. Hollander, K. Jon-And, P.-R. Kettle, P. Kokkas, R. Kreuger, R. L. Gac, F. Leimgruber, I. Mandić, N. Manthos, G. Marel, M. Mikuž, J. Miller, F. Montanet, A. Muller, T. Nakada, B. Pagels, I. Papadopoulos, P. Pavlopoulos, A. Policarpo, G. Polivka, R. Rickenbach, B. Roberts, T. Ruf, C. Santoni, M. Schäfer, L. Schaller, T. Schietinger, A. Schopper, L. Tauscher, C. Thibault, F. Touchard, C. Touramanis, C. V. Eijk, S. Vlachos, P. Weber, O. Wigger, M. Wolter, D. Zavrtanik, and D. Zimmerman (CPLEAR Collaboration), Phys. Lett. B **444**, 43 (1998).
[9] L. Wolfenstein, Int. J. Mod. Phys. E **08**, 501 (1999).
[10] J. Bernabeu, A. D. Domenico, and P. Villanueva-Perez, Nucl. Phys. B **868**, 102 (2013).
[11] J. P. Lees *et al.* (BABAR Collaboration), Phys. Rev. Lett. **109**, 211801 (2012).
[12] N. Cabibbo, Phys. Rev. Lett. **10**, 531 (1963).
[13] M. S. Sozzi, *Discrete Symmetries and CP Violation: From Experiment to Theory* (Oxford University Press, Oxford, UK, 2008).
[14] C. A. Baker, D. D. Doyle, P. Geltenbort, K. Green, M. G. D. van der Grinten, P. G. Harris, P. Iaydjiev, S. N. Ivanov, D. J. R. May, J. M. Pendlebury, J. D. Richardson, D. Shiers, and K. F. Smith, Phys. Rev. Lett. **97**, 131801 (2006).
[15] B. C. Regan, E. D. Commins, C. J. Schmidt, and D. DeMille, Phys. Rev. Lett. **88**, 071805 (2002).
[16] W. C. Griffith, M. D. Swallows, T. H. Loftus, M. V. Romalis, B. R. Heckel, and E. N. Fortson, Phys. Rev. Lett. **102**, 101601 (2009).
[17] J. J. Hudson, D. M. Kara, I. J. Smallman, B. E. Sauer, M. R. Tarbutt, and E. A. Hinds, Nature (London) **473**, 493 (2011).
[18] T. A. C. J. Baron, W. C. Campbell, D. DeMille, J. M. Doyle, G. Gabrielse, Y. V. Gurevich, P. W. Hess, N. R. Hutzler, E. Kirilov, I. Kozyryev, B. R. O'Leary, C. D. Panda, M. F. Parsons, E. S. Petrik, B. Spaun, A. C. Vutha, and A. D. West (ACME Collaboration), Science **343**, 269 (2014).
[19] J. S. M. Ginges and V. V. Flambaum, Phys. Rep. **397**, 63 (2004).
[20] *Advanced Series on Directions in High Energy Physics*, edited by B. L. Roberts and W. J. Marciano (World Scientific, Singapore, 2009), Vol. 20.
[21] V. A. Dzuba, V. V. Flambaum, and C. Harabati, Phys. Rev. A **84**, 052108 (2011).
[22] Y. Singh and B. K. Sahoo, Phys. Rev. A **91**, 030501 (2015).
[23] M. D. Swallows, T. H. Loftus, W. C. Griffith, B. R. Heckel, E. N. Fortson, and M. V. Romalis, Phys. Rev. A **87**, 012102 (2013).
[24] R. Eichler, N. V. Aksenov, A. V. Belozerov, G. A. Bozhikov, V. I. Chepigin, S. N. Dmitriev, R. Dressler, H. W. Gäggeler, V. A. Gorshkov, F. Haenssler, M. G. Itkis, A. Laube, V. Y. Lebedev, O. N. Malyshev, Y. T. Oganessian, O. V. Petrushkin, D. Piguet, P. Rasmussen, S. V. Shishkin, A. V. Shutov, A. I. Svirikhin, E. E. Tereshatov, G. K. Vostokin, M. Wegrzecki, and A. V. Yeremin, Nature (London) **447**, 72 (2002).
[25] R. C. Barber, H. W. Gäggeler, P. J. Karol, H. Nakahara, E. Vardaci, and E. Vogt, Pure Appl. Chem. **81**, 1331 (2009).
[26] K. G. Dyall, I. P. Grant, C. T. Johnson, F. A. Parpia, and E. P. Plummer, Comput. Phys. Commun. **55**, 425 (1989).
[27] P. Jönsson, G. Gaigalas, J. Bieroń, C. Froese Fischer, and I. P. Grant, Comput. Phys. Commun. **184**, 2197 (2013).
[28] B. J. McKenzie, I. P. Grant, and P. H. Norrington, Comput. Phys. Commun. **21**, 233 (1980).
[29] F. A. Parpia, C. Froese Fischer, and I. P. Grant, Comput. Phys. Commun. **94**, 249 (1996).
[30] I. P. Grant, Comput. Phys. Commun. **84**, 59 (1994).
[31] P. Jönsson, X. He, and C. Froese Fischer, Comput. Phys. Commun. **176**, 597 (2007).
[32] I. P. Grant, *Relativistic Quantum Theory of Atoms and Molecules: Theory and Computation* (Springer, New York, 2007).
[33] L. Radžiūtė, G. Gaigalas, P. Jönsson, and J. Bieroń, Phys. Rev. A **90**, 012528 (2014).
[34] J. Bieroń, C. Froese Fischer, P. Indelicato, P. Jönsson, and P. Pyykkö, Phys. Rev. A **79**, 052502 (2009).

[35] J. Bieroń, C. Froese Fischer, S. Fritzsche, G. Gaigalas, I. P. Grant, P. Indelicato, P. Jönsson, and P. Pyykkö, Phys. Scr. **90**, 054011 (2015).

[36] L. Radžiūtė, G. Gaigalas, D. Kato, P. Jönsson, P. Rynkun, S. Kučas, V. Jonauskas, and R. Matulianec, J. Quant. Spectrosc. Radiat. Transfer **152**, 94 (2015).

[37] G. Gaigalas, Z. Rudzikas, and C. Froese Fischer, J. Phys. B **30**, 3747 (1997).

[38] V. A. Dzuba, V. V. Flambaum, and S. G. Porsev, Phys. Rev. A **80**, 032120 (2009).

[39] V. V. Flambaum and J. S. M. Ginges, Phys. Rev. A **65**, 032113 (2002).

[40] R. D. Cowan and J. E. Hansen, J. Opt. Soc. Am. **71**, 60 (1981).

[41] P. Syty, J. Sienkiewicz, L. Radžiūtė, G. Gaigalas, and J. Bieroń (unpublished).

[42] U. Fano and J. W. Cooper, Rev. Mod. Phys. **40**, 441 (1965).

[43] A.-M. Mårtensson-Pendrill, Phys. Rev. Lett. **54**, 1153 (1985).

[44] K. V. P. Latha, D. Angom, R. J. Chaudhuri, B. P. Das, and D. Mukherjee, J. Phys. B **41**, 035005 (2008).

[45] K. V. P. Latha, D. Angom, B. P. Das, and D. Mukherjee, Phys. Rev. Lett. **103**, 083001 (2009).

[46] V. A. Dzuba, V. V. Flambaum, J. S. M. Ginges, and M. G. Kozlov, Phys. Rev. A **66**, 012111 (2002).

[47] V. A. Dzuba, V. V. Flambaum, and J. S. M. Ginges, Phys. Rev. A **76**, 034501 (2007).

[48] A.-M. Mårtensson-Pendrill and P. Öster, Phys. Scr. **36**, 444 (1987).

[49] A. Kramida, Yu. Ralchenko, J. Reader, and NIST ASD Team, http://physics.nist.gov/asd.

[50] G. Gaigalas, T. Žalandauskas, and Z. Rudzikas, At. Data Nucl. Data Tables **84**, 99 (2003).

[51] G. Gaigalas, T. Žalandauskas, and S. Fritzsche, Comput. Phys. Commun. **157**, 239 (2004).

[52] Y. J. Yu, J. G. Li, C. Z. Dong, X. B. Ding, S. Fritzsche, and B. Fricke, Eur. Phys. J. D **44**, 51 (2007).

[53] T. H. Dinh, V. A. Dzuba, and V. V. Flambaum, Phys. Rev. A **78**, 062502 (2008).

[54] R. Smolańczuk, Phys. Rev. C **56**, 812 (1997).

[55] V. Zagrebaev, A. Karpov, and W. Greiner, J. Phys.: Conf. Ser. **420**, 012001 (2013).

[56] http://www.nndc.bnl.gov/nudat2.

[57] B. Graner, Y. Chen, E. G. Lindahl, and B. R. Heckel, Phys. Rev. Lett. **116**, 161601 (2016).

[58] B. Fricke, W. Greiner, and J. T. Waber, Theor. Chim. Acta **21**, 235 (1971).

[59] R. A. Penneman, J. B. Mann, and C. K. Jørgensen, Chem. Phys. Lett. **8**, 321 (1971).

[60] P. Pyykkö, Phys. Chem. Chem. Phys. **13**, 161 (2011).

[61] C. Froese Fischer, T. Brage, and P. Jönsson, *Computational Atomic Structure: An MCHF Approach* (Institute of Physics Publishing, Bristol, UK, 1997).

[62] D. Layzer, Ann. Phys. **8**, 271 (1959).

[63] D. Layzer, Z. Horák, M. N. Lewis, and D. P. Thompson, Ann. Phys. **29**, 101 (1964).

[64] B. Edlén, *Handbuch der physik* (Springer, Berlin, 1964), p. 80.

[65] R. D. Cowan, *The Theory of Atomic Structure and Spectra* (University of California Press, Berkeley, CA, 1981).

[66] W. L. Wiese and A. W. Weiss, Phys. Rev. **175**, 50 (1968).

[67] M. A. Bouchiat and C. Bouchiat, J. Phys. **35**, 899 (1974).

[68] M. A. Bouchiat and C. C. Bouchiat, Phys. Lett. B **48**, 111 (1974).

[69] M. A. Bouchiat and C. Bouchiat, J. Phys. **36**, 493 (1975).

[70] O. P. Sushkov, V. V. Flambaum, and I. B. Khriplovich, Zh. Eksp. Teor. Fiz. **87**, 1521 (1984) [Sov. Phys. JETP **60**, 873 (1984)].

[71] I. B. Khriplovich, *Parity Nonconservation in Atomic Phenomena* (Gordon and Breach, New York, 1991).

[72] J. W. Rohlf, *Modern Physics from α to $Z = 112^0$* (Wiley, New York, 1994).

[73] W. Greiner, *Relativistic Quantum Mechanics—Wave Equations* (Springer-Verlag, Berlin, 1990).

[74] W. Greiner, *Quantum Electrodynamics* (Springer-Verlag, Berlin, 1994).

[75] P. Indelicato, J. Bieroń, and P. Jönsson, Theor. Chem. Acc. **129**, 495 (2011).

[76] I. Goidenko, I. Tupitsyn, and G. Plunien, Eur. Phys. J. D **45**, 171 (2007).

[77] U. Dammalapati, K. Jungmann, and L. Willmann, J. Phys. Chem. Ref. Data **45**, 013101 (2016).

[78] J. M. Amini, C. T. Munger, Jr., and H. Gould, Phys. Rev. A **75**, 063416 (2007).

[79] M. V. Romalis, W. C. Griffith, J. P. Jacobs, and E. N. Fortson, Phys. Rev. Lett. **86**, 2505 (2001).

[80] C. E. Wieman, D. E. Pritchard, and D. J. Wineland, Rev. Mod. Phys. **71**, S253 (1999).

[81] S. De, U. Dammalapati, and L. Willmann, Phys. Rev. A **91**, 032517 (2015).

[82] D. J. Wineland, Rev. Mod. Phys. **85**, 1103 (2013).

[83] A. D. Ludlow, M. M. Boyd, and J. Ye, Rev. Mod. Phys. **87**, 637 (2015).

[84] R. H. Parker, M. R. Dietrich, M. R. Kalita, N. D. Lemke, K. G. Bailey, M. N. Bishof, J. P. Greene, R. J. Holt, W. Korsch, Z.-T. Lu, P. Mueller, T. P. O'Connor, and J. T. Singh, Phys. Rev. Lett. **114**, 233002 (2015).

[85] B. Cheal and K. T. Flanagan, J. Phys. G: Nucl. Part. Phys. **37**, 113101 (2010).

[86] Y. Oganessian, J. Phys.: Conf. Ser. **337**, 012005 (2012).

[87] S. Sasmal, H. Pathak, M. K. Nayak, N. Vaval, and S. Pal, J. Chem. Phys. **144**, 124307 (2016).

[88] A. Sunaga, M. Abe, M. Hada, and B. P. Das, Phys. Rev. A **93**, 042507 (2016).

[89] E. B. Norrgard, D. J. McCarron, M. H. Steinecker, M. R. Tarbutt, and D. DeMille, Phys. Rev. Lett. **116**, 063004 (2016).

[90] A. Prehn, M. Ibrügger, R. Glöckner, G. Rempe, and M. Zeppenfeld, Phys. Rev. Lett. **116**, 063005 (2016).

[91] T. A. Isaev and R. Berger, Phys. Rev. Lett. **116**, 063006 (2016).

[92] C. D. Panda, B. R. O'Leary, A. D. West, J. Baron, P. W. Hess, C. Hoffman, E. Kirilov, C. B. Overstreet, E. P. West, D. DeMille, J. M. Doyle, and G. Gabrielse, Phys. Rev. A **93**, 052110 (2016).

[93] T. Fleig, M. K. Nayak, and M. G. Kozlov, Phys. Rev. A **93**, 012505 (2016).

[94] A. E. Leanhardt, J. L. Bohn, H. Loh, P. Maletinsky, E. R. Meyer, L. C. Sinclair, R. P. Stutz, and E. A. Cornell, J. Mol. Spectrosc. **270**, 1 (2011).

[95] D. N. Gresh, K. C. Cossel, Y. Zhou, J. Ye, and E. A. Cornell, J. Mol. Spectrosc. **319**, 1 (2016).

[96] Attributed to Robert H. Goddard.